Chapter 7 Friction, wear, and failure performance enhancement of Karanja oil by chemically-functionalized hexagonal boron nitride

This study explores ways to improve the lubrication properties of pure Karanja oil by modifying it with fractional epoxidation and adding chemically-modified hexagonal boron nitride (h-BN) nanosheets. The process begins with blending epoxidized oil into the pure Karanja oil to enhance its lubricating performance. The resulting oil blends are then tested using the Stribeck curve under constant load and varying speeds, which reveals that the lubrication mostly operates in the boundary regime at lower speeds. To further boost the oil's performance, environmentally friendly h-BN nanosheets are added, improving the oil's load-carrying capacity. The study follows ASTM D 5183 standards for lubrication testing, examining how well the lubricant blends perform under contact stress and comparing their behaviour until they reach the point of failure. The goal is to understand how the oil modification and nano-additives impact tribological performance and load-bearing abilities, shedding light on their potential for improving lubrication in practical applications.

7.1. Oil characterization

7.1.1. FTIR of modified oil

Figure 7.1 shows the FTIR spectroscopic analysis of Karanja oil across different stages of its purification and modification. The spectra for cold-pressed raw Karanja oil and degummed Karanja oil reveal similar peaks, including those in the C-H regions. This indicates that the primary chemical composition of the oil remains unchanged after the degumming process. However, during epoxidation, the peak at 3006 cm^{-1} weakens, reflecting the reduction of the unsaturated -CH=CH- bonds in this reaction [119].

Additionally, a new peak appears at 826 cm^{-1}, signifying the formation of C-O-C linkages as a result of epoxidizing the double bonds of oil contents. These changes confirm that the unsaturated bonds in the Karanja oil have been successfully converted during the epoxidation process.

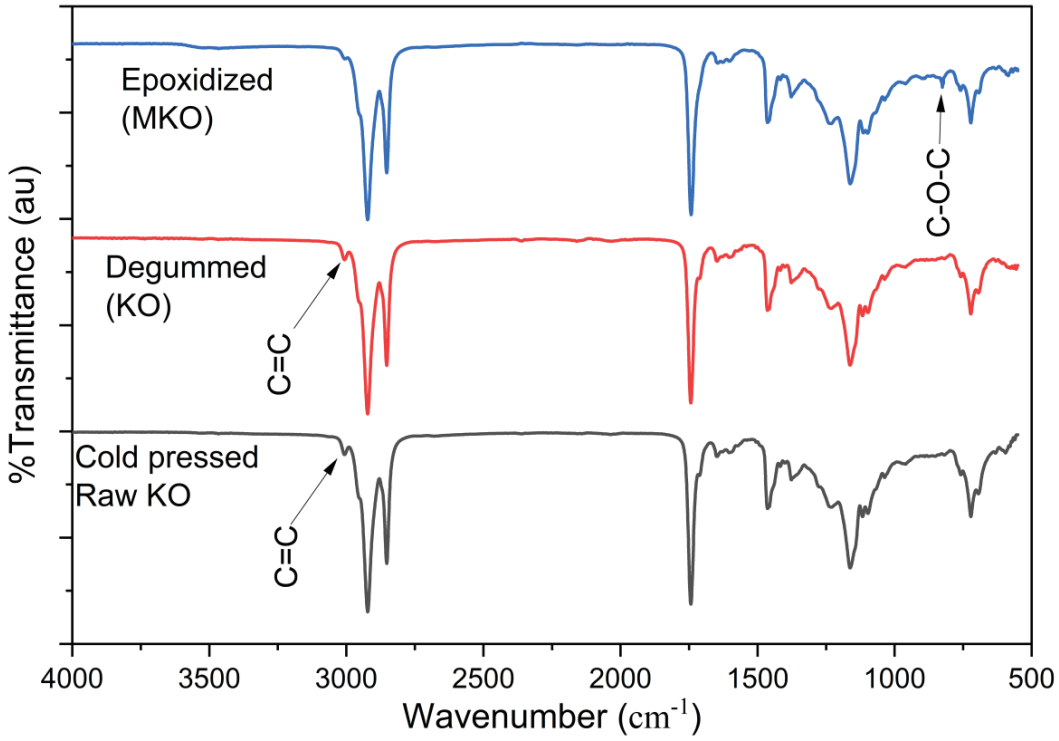

Figure 7.1 FTIR spectra of Karanja oil at different stages of modifications

7.1.2. ^{1}H NMR of oil

The ^{1}H NMR spectra confirm a substantial reduction in the unsaturation of Karanja oil after epoxidation. As depicted in Figure 7.2, the spectrum of raw Karanja oil reveals three characteristic chemical shifts corresponding to specific unsaturated structural groups: 5.32–5.37 ppm for olefinic (-CH=CH-) bonds, 2.77 ppm for diallylic methylene (-CH=CH-CH_2-CH=CH-), and 1.99–2.05 ppm for allylic methylene (-CH_2-CH_2-CH=CH-) groups, labelled as a, b, and c, respectively. These peaks represent the oil's original unsaturated bonds. After epoxidation, the normalized integral intensities of these

chemical shifts decrease significantly by 53-55%, indicating a marked reduction in unsaturation. This substantial decline demonstrates that a large proportion of the unsaturated bonds in raw Karanja oil have been successfully modified, likely due to oxygen incorporation during the epoxidation process. These chemical changes enhance the oil's stability and functionality, making it more suitable for industrial applications.

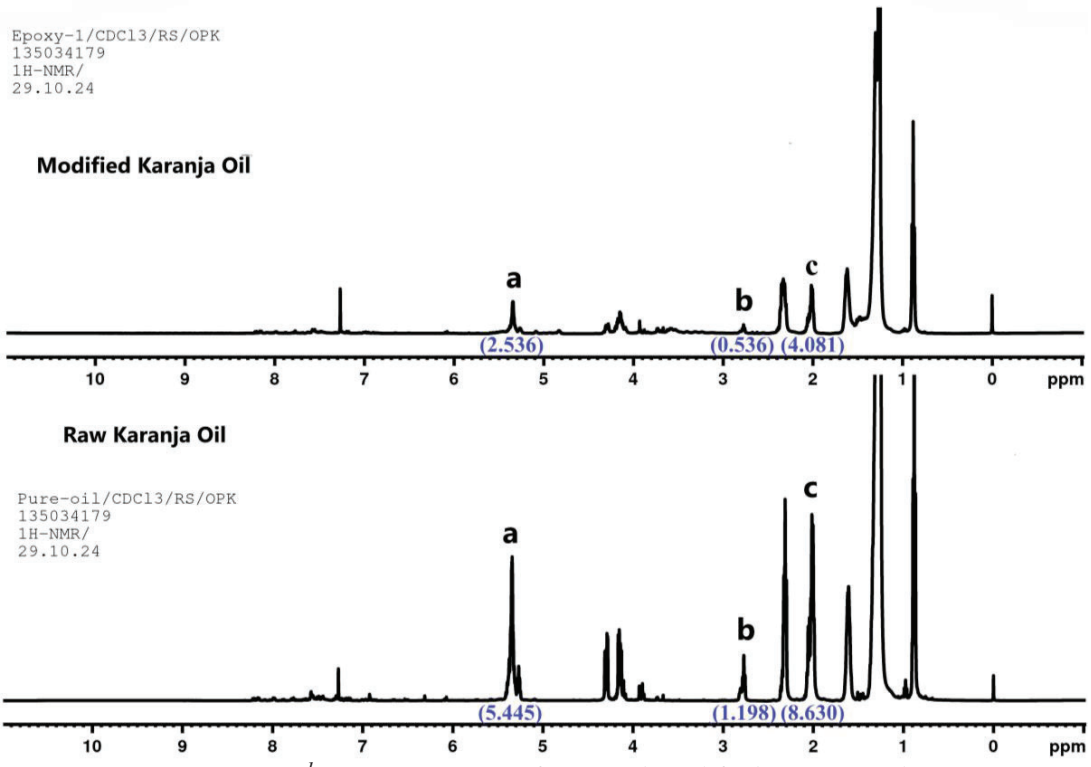

Figure 7.2 [1]H-NMR spectra of raw and modified Karanja oils

7.2. Characterization of nanoparticles

7.2.1. X-ray diffraction results of particles

Figures 7.3 (a) and (b) display the X-ray diffraction patterns for hexagonal boron nitride (h-BN) and functionalized hexagonal boron nitride (fh-BN). The XRD peaks observed at diffraction angles of 26.67°, 41.55°, 43.60°, 50.06°, 54.99°, and 75.86° correspond to the (002), (100), (101), (102), (004), and (110) lattice planes of h-BN, aligning with the ICSD reference code 01-073-2095 for hexagonal boron nitride [120] (Figure 7.3(a)). In Figure 7.3(b), the XRD pattern for fh-BN shows peaks that match those of h-BN, with the

exception of a broad, amorphous peak at around 22°, attributing to the formation of an amorphous silica/carbon-like material. This peak is quantified at 3% based on the XRD analysis, indicating that a new substance was produced during the modification process.

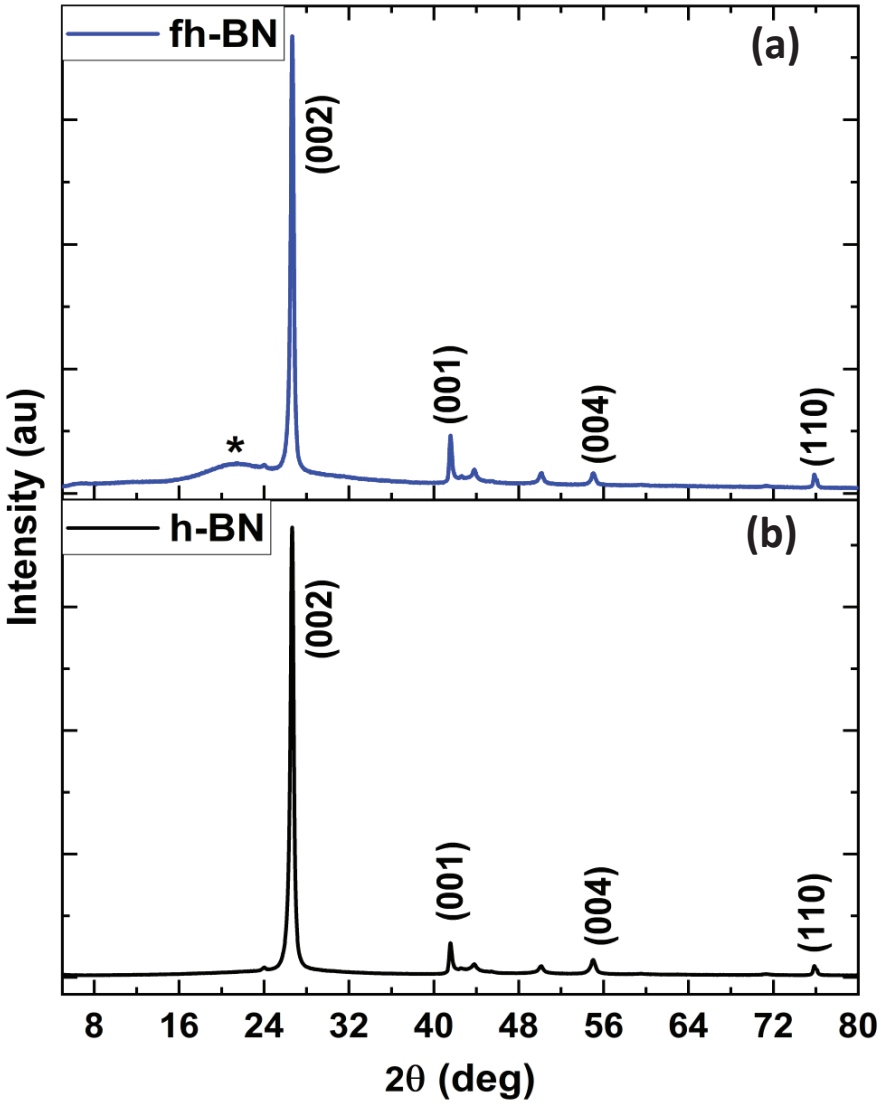

Figure 7.3 XRD Spectra of (a) f-h-BN, (b) h-BN

Previous research by Yang et al. [121] found that when carbon is grafted onto h-BN, a peak appears around 25°. In our case, however, a fatty acid layer is applied over the h-BN, and further analysis is needed to confirm the exact nature of the functionalized material and the presence of fh-BN.

7.2.2. Raman characteristics of h-BN and fh-BN

The Raman spectra (Figure 7.4) show the vibrational characteristics of h-BN and fh-BN. For h-BN, there's a strong peak at 1364 cm^{-1}, attributing to the E2g vibrational mode of the h-BN nanosheets [122]. This mode represents the in-plane vibrations of the boron and nitrogen atoms within the hexagonal structure of h-BN, and it typically appears as an intense and sharp peak[123].

On the other hand, the Raman spectrum of fh-BN shows a slight broadening and a shift to lower wavelengths (red shift) for the E2g peak. This change is attributed to the structural strain that induced by interaction with APTMS with the B-N bonds in the h-BN structure. Essentially, the functionalization process slightly induces structural strain, which is

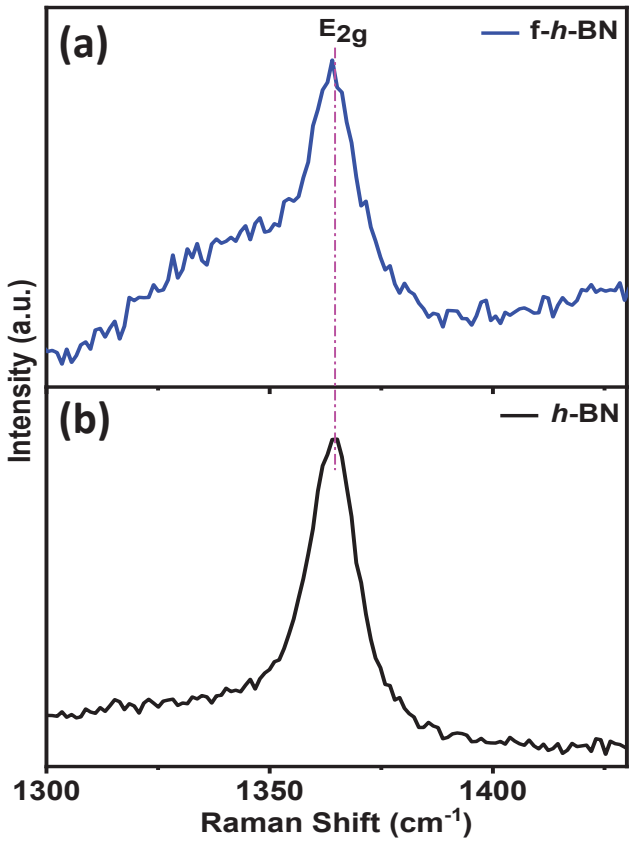

Figure 7.4 Raman spectra of (a) h-BN and (b) fh-BN, demonstrating the E2g band reflected in the Raman spectra in the form of a broader and shifted peak.

7.2.3. FTIR of hybrid additives

Figure 7.5 presents the FTIR spectra for both h-BN and fh-BN, offering a closer look at the vibrational characteristics of these materials. For h-BN, there's a sharp peak at 807 cm^{-1}, which corresponds to the out-of-plane bending of the B-N bonds, while a broad, strong peak at 1390 cm^{-1} indicates the in-plane stretching of these bonds [124]. Another significant peak appears around 3404 cm^{-1}, which is associated with hydroxyl groups on the surface of h-BN, suggesting the presence of surface-bound hydroxyl functionalities or water molecules.

Additionally, at 1038 cm^{-1}, a signal is detected that corresponds to the Si-O stretching vibration, indicating the formation of an APTMS (aminopropyltriethoxysilane) layer on the surface of the h-BN nanosheets [125]. This is further confirmed by the appearance of two peaks at 1198 and 695 cm^{-1}, which are related to the C-N stretching and N-H wagging modes, respectively signals of APTMS grafting onto the h-BN surface.

In the case of fh-BN, we also see two new peaks around 2927 and 2853 cm^{-1}. These peaks are attributed to the asymmetric and symmetric vibrations of the methylene group, confirming the presence of a fatty acid layer on the surface of the h-BN nanosheets [126]. This suggests that the h-BN has been functionalized with a fatty acid after sonication, which helps to form the modified fh-BN, a process similar to what was observed in Vu's work [127].

In addition, a small peak around 1035 cm^{-1} in the fh-BN spectrum is attributed to the Si-O-Si stretching vibrations. This suggests that some polymerization of APTMS has occurred during the reaction, forming a partially polymerized APTMS on the h-BN surface. This also helps explain the unknown peak seen at 22 degrees in the XRD spectrum, which is now understood to correspond to this polymerized silica. All these

findings support the idea that the h-BN nanosheets have been successfully functionalized with both APTMS and fatty acid layers.

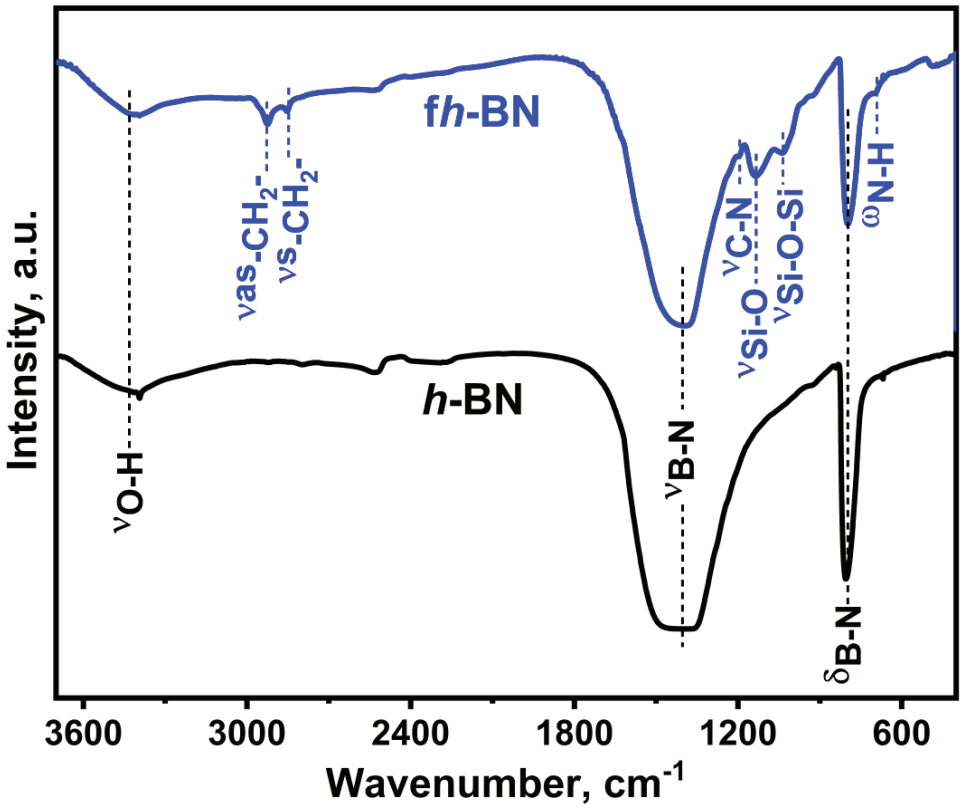

Figure 7.5 FTIR spectra of h-BN and fh-BN along with the characteristic's vibrational features

7.2.4. Dispersion of nanoparticles

Functionalized 2D sheets of h-BN shows better dispersion stability as compared to pristine h-BN depicted in Figure 7.6. The functionalized additives show dispersion for 6 days but in case of pristine h-BN there is a settlement of particles at the bottom of the vial. The functionalization of sheets with the molecules of modified oil increases steric stabilization effect and thus improving stability.

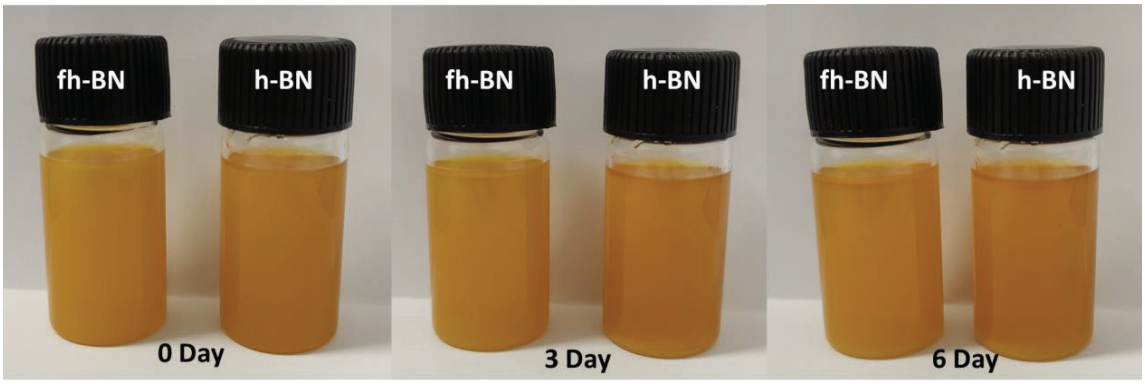

Figure 7.6 Digital images of dispersion of nanolubricants functionalized h-BN fh-BN and h-BN

7.2.5. Morphological studies

High-resolution transmission electron microscopy (HRTEM) and field emission scanning electron microscopy (FESEM) were used to study the morphological features of h-BN and functionalized h-BN (fh-BN). The HRTEM images of both h-BN (Figure 7.7(a)) and fh-BN (Figure 7.7(d)) reveal a flat, sheet-like structure, typical of materials that have a two-dimensional form. Both types of materials have a lamellar structure, with about 10 to 15 layers stacked with each other via van der Waals interaction. The selected area electron diffraction (SAED) patterns of both h-BN and fh-BN confirm that they are polycrystalline, meaning they have many small crystalline regions within their structure. The FESEM images (Figures 7.7(g) and 7.7(h)) further support the flat, sheet-like appearance seen in the HRTEM images, confirming the consistent structure of both h-BN and fh-BN.

To assess the particle size, the dimensions of 30 randomly selected particles were measured in two perpendicular directions using the SEM images. The average particle size of h-BN was found to be 156.2 nm, but after functionalizing it with APTMS and MKO, the particle size increased to 163.1 nm. This size increase suggests that a thin layer has formed on the surface of the h-BN sheets as a result of the functionalization process.

This layer, created by the combined action of APTMS and MKO, likely contributes to the enhanced dispersion of fh-BN.

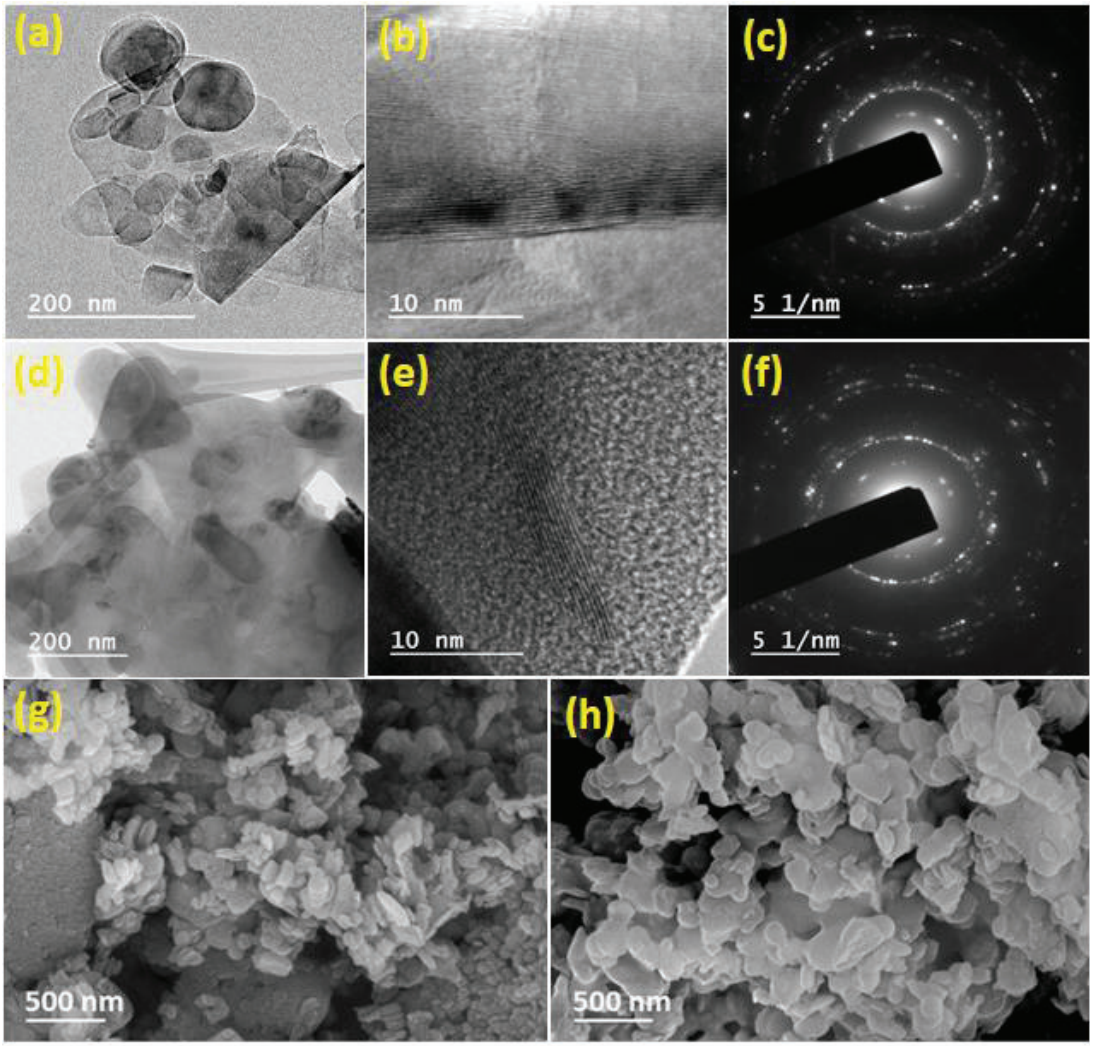

Figure 7.7 HRTEM images of (a, b) h-BN, (d, e) fh-BN, SAED pattern of (c) h-BN, (f) fh-BN, and FESEM images of (g) h-BN, and (h) fh-BN

7.3. Base oil blends and their rheology

The base oil used in this study is pure Karanja oil, which is blended with modified oil (MKO) in varying volume percentages from 0 to 100%, with increments of 25%. Viscosity measurements were taken at different temperatures for these blends using a rotational viscometer, as shown in Figure 7.8(a). The results show a clear trend where

viscosity decreases as the temperature rises. Among the blends, the one with the highest amount of modified oil (100% MKO) experiences the most significant drop in viscosity, while the pure Karanja oil shows the least change. As the percentage of MKO increases in the blend, the viscosity of the mixture also rises, likely due to the epoxidation of the oil[128].

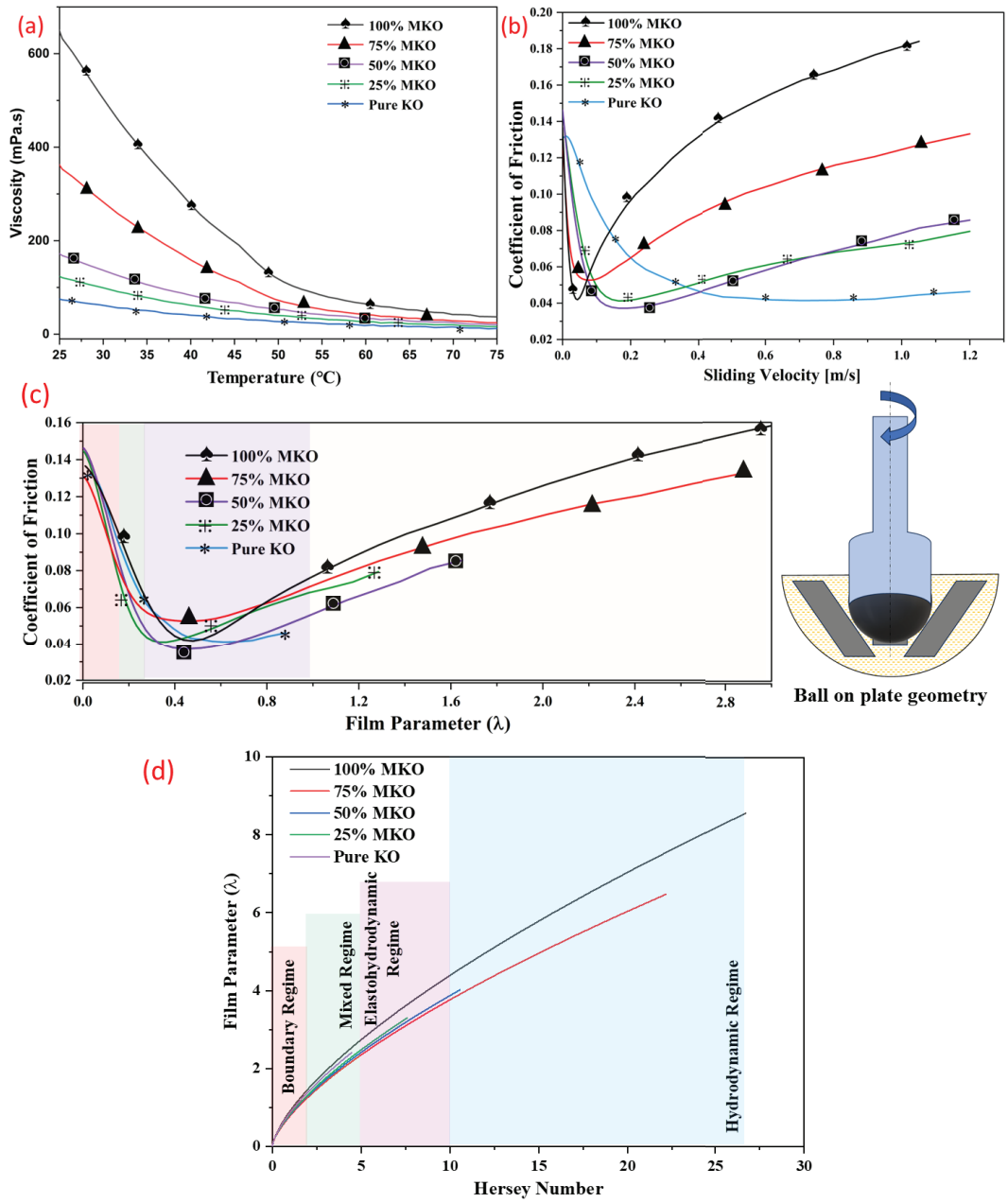

Figure 7.8 Base oil and their blend properties (a) dynamic viscosity at various temperatures using rotational type viscometer, (b) coefficient of friction at different sliding velocities at room temperature, and (c) coefficient of friction with film parameter(λ) at room temperature with testing geometry (d) Dimension less film parameter and Hersey number plot for the lubricant and its modified blend

Figure 7.8(b) presents a plot of the coefficient of friction (COF) versus sliding speed, measured under a 5 N load at various speeds using a ball-on-plate geometry and an MCR 102 rheometer at room temperature. The results show that the 50% MKO blend has the lowest coefficient of friction between speeds of 0.1 and 0.4 m/s. In contrast, pure Karanja oil and the 100% MKO blend had the highest friction in this range. Interestingly, at speeds below 0.05 m/s, the 100% modified oil showed the lowest COF, although at higher speeds, its COF becomes higher, even with similar film parameters to other blends (as shown in Figure 7.8(c)). Whereas Figure 7.8 (d) shows the separate lubrication regimes according to the Hersey number ($\eta\omega/p$) where η is dynamic viscosity ω is the angular velocity and p is load which is constant 5 N for this case.

The film parameter, which is a dimensionless number, represents how well the lubricant film separates the surfaces. For pure Karanja oil, the film parameter values are below one ($\lambda<1$), while the blends have higher values. This suggests that the modified oil blends, with their higher oxirane ring content, form a thicker film at lower speeds, reducing friction by minimizing direct contact and shear stress[129]. However, as speed increases, the fluid's viscosity becomes more significant, causing higher shear stress due to increased motion between the fluid layers, which results in greater friction.

Figure 7.8(c) shows the relationship between the COF and the film parameter, which is the ratio of the minimum film thickness to the equivalent roughness of the surface. The film parameter is calculated using the Hamrock equation, as discussed in Chapter 3[130], and is supported by data from ISO/TR 1281-2:2008. The results indicate that blends containing 25% to 50% MKO are effective in reducing friction within the tested speed range. The curve also shows that these blends have a higher film parameter than pure oil at the same speeds.

To better understand the effect of nano additives, the lubrication regime must remain within the boundary regime. This can only be achieved with the lowest viscosity oils in this speed range, as shown in Figure 7.8(c). To further explore the impact of nano additives, pure Karanja oil is compared to the modified oil blends with varying percentages of MKO.

7.4. Tribological study

7.4.1. Fully flooded condition

The tribological properties of the oil were tested using a four-ball setup, following ASTM D 5183 guidelines. In this tribo test, the oil was for an hour at 75°C and 600 rpm, and then the wear scar diameters were measured. The ball pot containing the clamped balls was cleaned for further testing.

Next, a second test was conducted using the worn balls. The load was set to 10 kgf initially, then increased by 10 kgf every 10 minutes without stopping the machine. The coefficient of friction was measured at the end of each interval, and the test continued until signs of seizure appeared. This test provided insights into the oil's frictional behaviour and allowed a comparison of load-bearing capacity between different samples, based on the load at which seizure occurred.

Figure 7.9(a) shows that pure Karanja oil, as well as blends with 50% and 100% MKO (Modified Karanja Oil), and 0.025 wt% added h-BN (hexagonal Boron Nitride) and fh-BN (functionalized h-BN), all exhibited stable lubrication behaviour throughout the test. However, the blends with 25% and 75% MKO were unstable under varying loads. The failure points were found at 130 kgf for pure Karanja oil, 140 kgf for 25% MKO, 160 kgf for 0.025 wt% h-BN, 230 kgf for 50% MKO, 240 kgf for 75% MKO, 290 kgf for 0.025 wt% fh-BN, and 300 kgf for 100% MKO.

In Figure 7.9(b), the average coefficient of friction was higher for the 25% and 75% MKO blends, likely due to the interaction between the epoxidized fatty acids and the unsaturated bonds in the pure oil. The 50% MKO blend, which maintains a 1:1 ratio of oxirane to unsaturated bonds, shows better compatibility, resulting in the lowest coefficient of friction. Additionally, as the amount of modified oil increases, the wear volume decreases steadily. Interestingly, the 0.025 wt% fh-BN blend exhibited better antiwear properties than pure h-BN. This could be because the oxirane functional group has a stronger affinity for the metal surface, and the stable dispersion of fh-BN improves the oil's performance. TEM images show that h-BN particles have a lamellar (layered) structure. These layers can slide over each other, creating a slippery surface that reduces friction between moving parts[131]. When added to a lubricant, h-BN acts as a solid lubricant, reducing direct contact and friction between surfaces. Functionalized h-BN particles can form a protective coating on metal components, acting as a barrier and preventing wear caused by friction. The functionalization process improves the interaction between the nanoparticles and the metal surface, making fh-BN more effective than unmodified h-BN.

The tests were performed in a fully flooded condition, so replenishment wasn't a concern due to the ample lubrication in the cup. However, if the lubricant level drops, the supply to the contacting surfaces decreases, leading to scuffing failure [132]. When the lubricant level drops, it can cause metal-to-metal contact, leading to increased wear and surface damage[133].

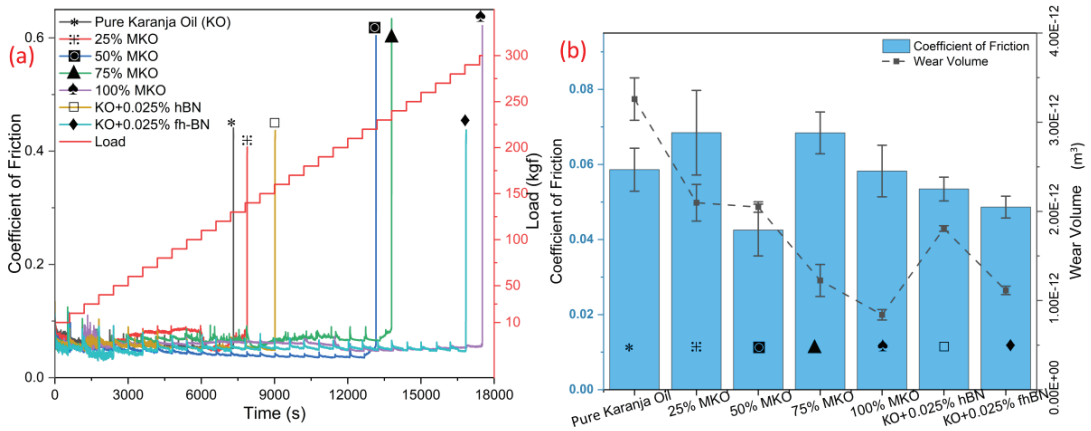

Figure 7.9 (a) Coefficient of friction versus time curve for different lubricated oil blends, (b) Wear volume and average coefficient of friction for different lubricants used. (ASTM D5183)

7.4.2. Starved lubrication

The experiments were carried out at room temperature under a lubricated system with limited lube oil (starving conditions) and reciprocating sliding. A Multi-Function Tribometer (MFT) was used to compare the performance of various lubricants in these challenging conditions. About 2 to 3 µl of each lubricant was applied to a flat disc made of 100Cr6 bearing steel with an average roughness of 0.21 µm. A 6 mm AISI 52100 steel ball served as the counter body during the tribological tests. The system was subjected to a 50 N load at a sliding speed of 0.1 m/s, with a 5 mm track length.

As shown in Figure 7.10(a), the 50% MKO blend performed the best among all the lubricants tested, followed closely by the 0.025 wt% fh-BN blended Karanja oil. This suggests that certain lubricant formulations are more effective in starvation conditions, providing lower friction and superior performance compared to other blends or additives. Figures 7.7(b) and 7.9(a) further support that the 50% MKO blend outperforms others in both fully flooded and starved lubrication conditions.

Figure 7.10(b) compares friction force (in Newton) versus the sliding distance (in mm) over 100 cycles of reciprocating sliding after 10 minutes of running. When the sliding motion occurs in the positive x-direction, the friction force is shown as negative, and it is positive in the opposite direction. The hysteresis plot generated from these results provides insight into the frictional effort during the sliding cycles. The area under the curve is integrated to determine the absolute frictional energy per cycle, expressed in N.mm.

The 50% MKO blend and 0.025 wt% fh-BN in Karanja oil significantly reduced frictional loss, as seen by the lower frictional energy per cycle. This indicates that these formulations offer more effective lubrication, reducing friction and improving performance during the reciprocating sliding tests compared to the other lubricants tested.

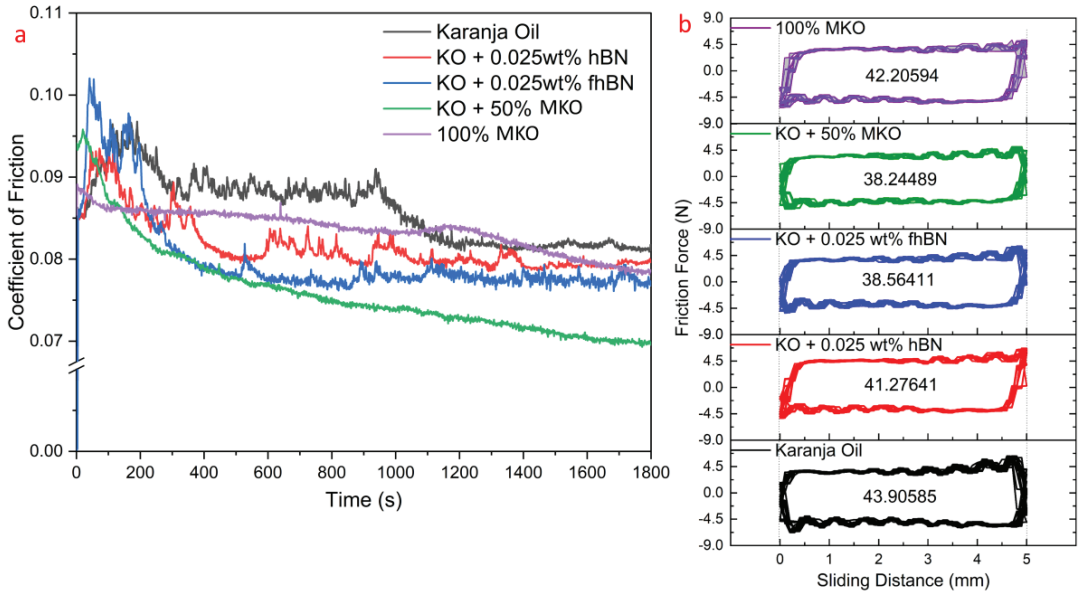

Figure 7.10 Starved lubrication test at Room Temperature (25 ℃) 5 mm stroke length at 10 Hz frequency (a) Coefficient of friction as a function of time for different oil samples, (b) Friction hysteresis plot of 100 cycles with area per cycle (in N.mm) after 10 min of running-in.

7.5. Worn surface study

The s from the sliding reciprocating tests were analysed using scanning electron microscopy (SEM), with images captured at various magnifications shown in Figure 7.11. Additionally, the worn surface profiles, measured perpendicular to the sliding direction using a surface profilometer, are presented in Figure 7.12 (a)–(e), while specific wear rate and corresponding film thickness are depicted in Figure 7.12 (f). The film thickness was calculated using the Hamrock equation, with viscosity data obtained from the viscometer at room temperature. Among the lubricants tested, the one containing 100% modified Karanja oil exhibited the lowest wear rate and the highest film thickness. Notably, a lubricant blend with 50% modified oil and 0.025 wt% fh-BN in Karanja oil showed wear rate comparable to those of the 100% modified oil. This indicates that adding fh-BN to Karanja oil achieves antiwear performance similar to that of a higher concentration of modified oil alone.

The inclusion of oxirane groups in the modified oil plays a key role, as these groups facilitate the formation of a stable protective layer over the metal surface during sliding, thereby enhancing the lubricant's antiwear properties. Furthermore, a comparison of pristine h-BN and fh-BN revealed that the functionalized variant performs better. This improvement stems from fh-BN’s ability to form a stronger and more robust layer on the tribo-surfaces,[134] which provides superior load-carrying capacity and reduces wear rate, as shown in Figure 7.9(a). Similar trends were observed under both fully flooded and starved lubrication conditions for fh-BN and h-BN systems as well as for modified oil blends. However, under fully flooded conditions, h-BN lubrication demonstrated better antiwear performance than under starved conditions. This is attributed to the higher availability and continuous replenishment of the nano-lubricant in fully flooded systems, which enhances its effectiveness in reducing wear rate.

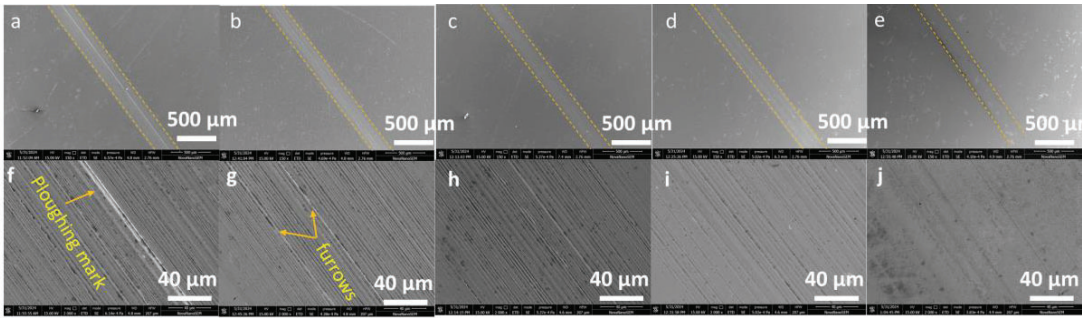

Figure 7.11 Worn tracks of the tribo-surfaces after reciprocating sliding test with (a, f) Pure Karanja oil, (b, g) 0.025 wt% h-BN +KO, (c, h) 0.025 wt% fh-BN + KO, (d, i) 50% MKO, (e, j) 100% MKO

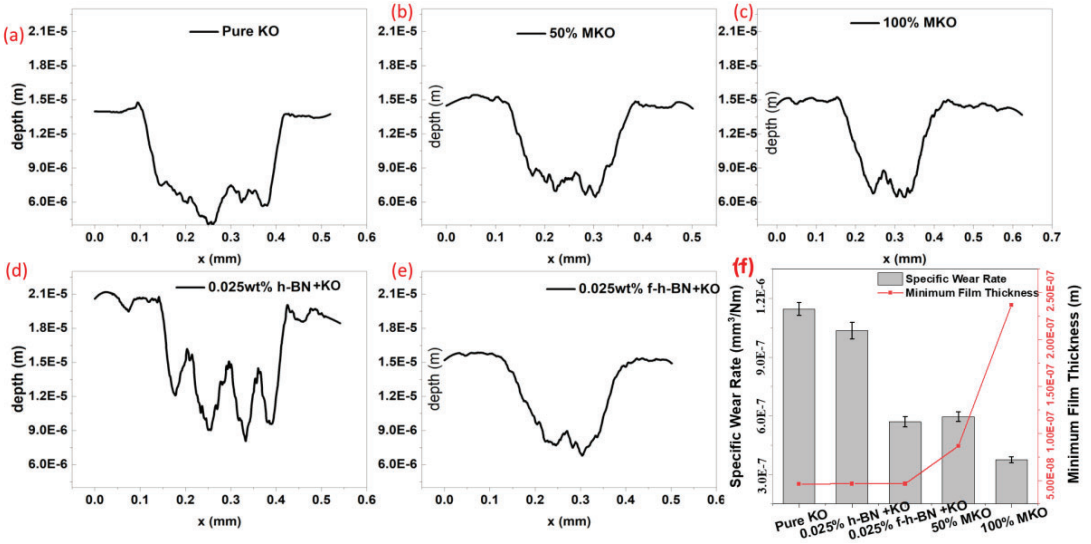

Figure 7.12 (a) to (e) Worn profile of different worn surface and (f) Specific wear rate for different lubricated tests measured from average area of the worn profile taken at three different places by stylus type surface profilometer with corresponding film thickness

7.6. Friction induced vibration at failure

The vibration patterns recorded during the tribological tests provide fascinating insights into how different lubricants behave under stress. The tests were conducted using three types of lubrication: pure oil, oil mixed with 0.025 wt% h-BN, and oil containing fh-BN. The results, shown in Figure 7.13 for the case of pure Karanja oil test, capture the

vibration signatures over time, starting from the beginning of the test. To dig deeper into the frequency content of these vibrations, the signals were analysed using a short-term Fourier transform (STFT), which converts the data into frequency-time graphs. These are presented in Figure 7.13 with focus on a 14-second interval along with the corresponding wear marks associated on the worn surface. While Figure 7.14 shows the results of h-BN lubricated surface and Figure 7.15 shows the results of friction induced vibration associated with fhBN.

The STFT graphs reveal distinct vibration frequencies at 4000 Hz, 2500 Hz, and below 1500 Hz across all tests. However, when nanoparticles are added to the lubricants, the amplitude of these frequencies changes noticeably. In particular, the presence of nanoparticles boosts the energy at frequencies between 1000–1500 Hz and 4000 Hz, highlighting their role in altering the lubricant's vibration behaviour.

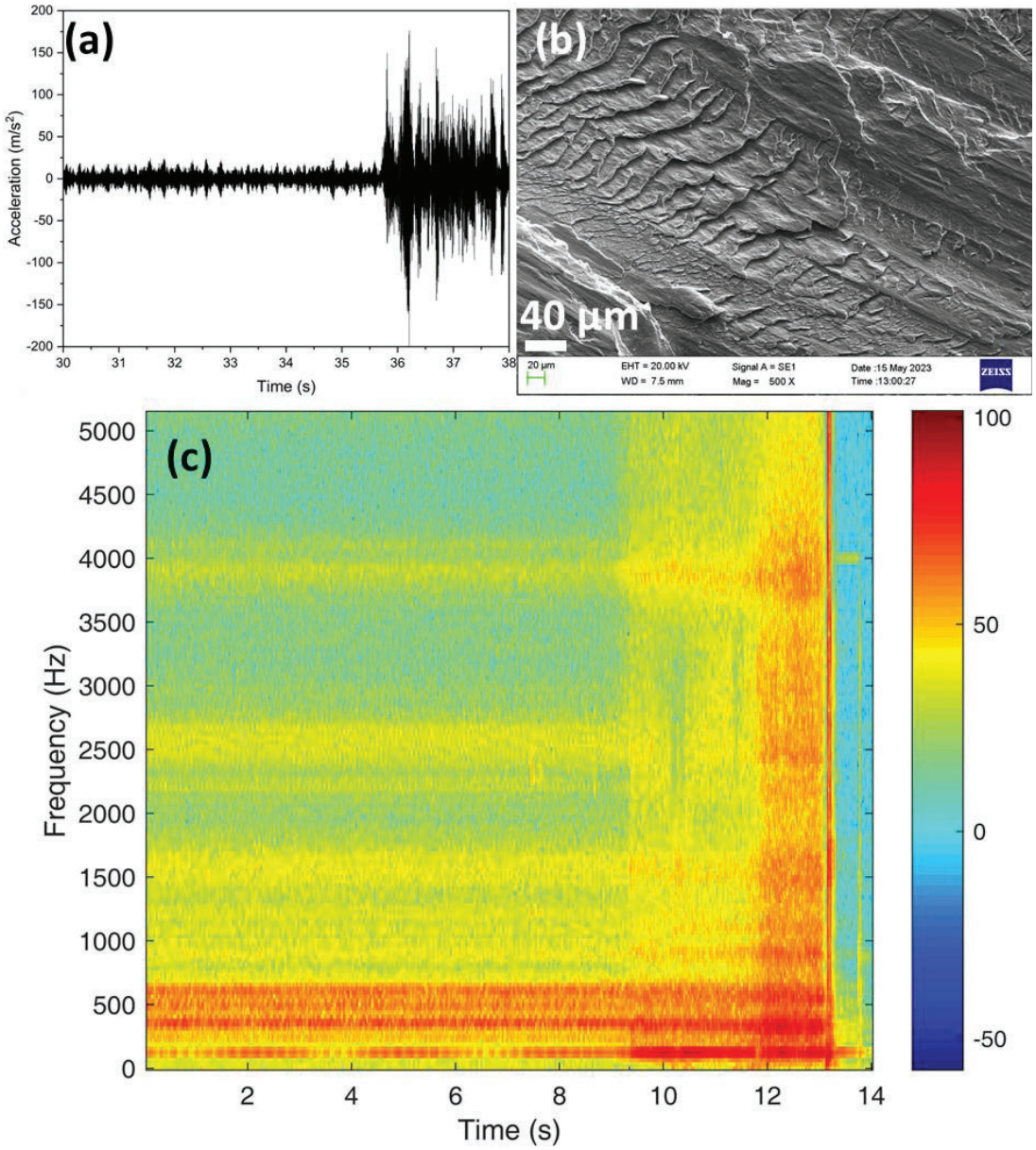

Figure 7.13 (a) The vibration signatures over time, (b) worn surface along with (c) STFT for pure Karanja oil

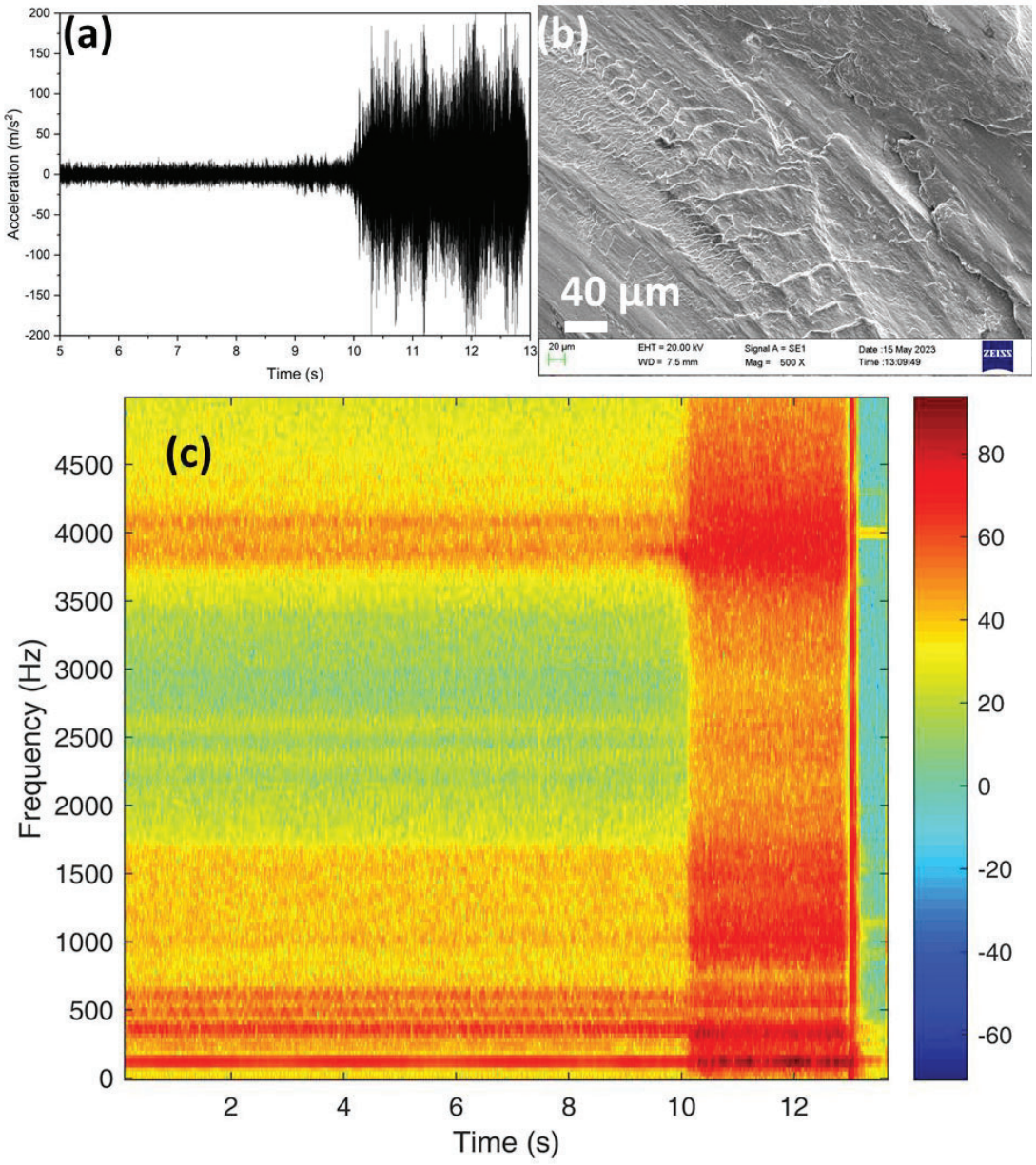

Figure 7.14 (a) The vibration signatures over time, (b) worn surface along with (c) STFT for 0.025% hBN + Karanja oil

When subjected to higher loads, nanoparticle-assisted lubrication starts to fail, leading to an increased frictional force. For pure oil, failure occurs suddenly around 10 seconds, marked by a sharp rise in vibration amplitude. This abrupt failure generates more energy at certain frequencies, which can be seen in the STFT graph (Figure 7.13, 7.14, 7.15) as a shift from yellow to red. Alongside this, the system's frequency range expands, creating

noise that signals severe surface damage and wear. In contrast, lubricants containing nanoparticles both h-BN and fh-BN exhibit a different failure pattern. Instead of a gradual increase, a sudden burst of energy appears, shown as a red band in STFT of Figures 7.13 and 7.14. This suggests that nanoparticle-based lubricants form a stable protective layer, which delays the onset of catastrophic wear.

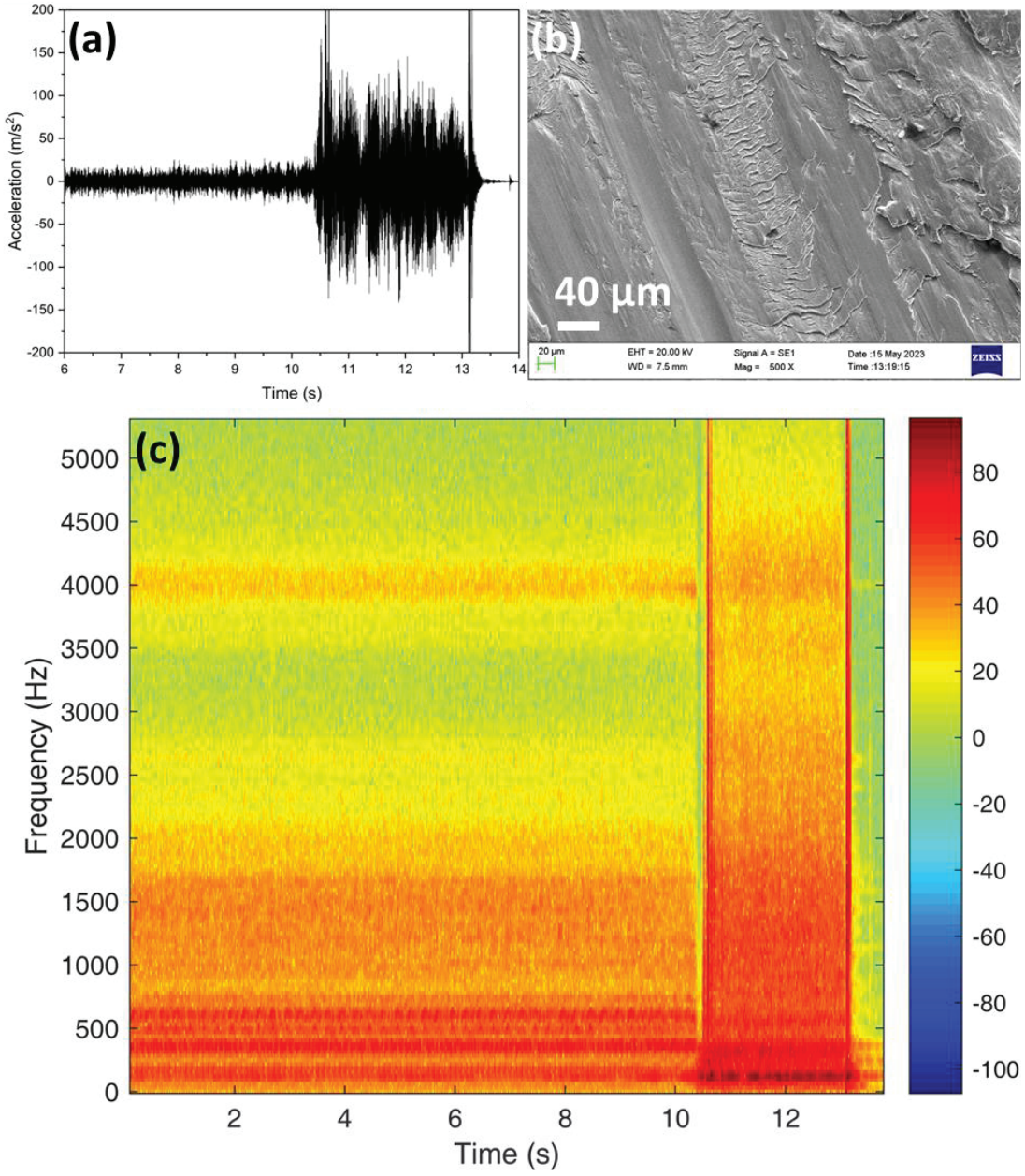

Figure 7.15 The vibration signatures over time, worn surface along with STFT for 0.025% fhBN + Karanja oil

Among these, fh-BN stands out. It shows a distinct ability to differentiate between regular vibrations and those signalling failure. This is due to the formation of a glazed layer on the surface, which momentarily halts sliding and protects the machine. However, when this layer eventually breaks, the system resumes sliding with a noticeable squeak. This behaviour demonstrates that functionalized nanoparticles can create a tough, stable film that supports heavy loads as long as the layer remains intact. This makes them particularly effective for extending the performance of less capable base oils like KO (kerosene oil).

Further insights come from SEM images of the worn surfaces, shown in top right corner of Figures 7.13, 7.14 and 7.15. These images reveal stepped ridges caused by adhesive wear, which vary in size depending on the lubricant used. Pure oil produces the largest ridges, indicating significant wear. On the other hand, fh-BN lubrication results in much smaller ridges, showing its superior ability to reduce wear. The surfaces lubricated with h-BN fall somewhere in between, with moderately sized ridges.

These variations highlight how stable nano-lubricants like fh-BN reduce surface adhesion, enabling smoother sliding even in harsh conditions. However, it's worth noting that h-BN doesn't perform as effectively due to agglomeration, where nanosheets clump together and disrupt their ability to form a uniform protective layer [135].

Overall, these findings point to the exciting potential of functionalized h-BN. By enhancing the stability and load-bearing capacity of lubricating films, fh-BN offers a reliable way to minimize wear, delay failure, and improve the performance of lubricants under extreme conditions.

7.7. Chapter summary

This chapter presents a comprehensive evaluation of the tribological behavior of Karanja Oil (KO) and its chemically modified form (MKO), with a focus on their performance under varying lubrication regimes. The modification of KO via epoxidation introduces oxirane functional groups, which enhances the oil's polarity and its affinity for metallic surfaces, thereby improving friction-reducing capabilities. However, the structural changes also result in a reduced viscosity index, making MKO more sensitive to temperature fluctuations and potentially limiting its usability in applications requiring thermal stability.

Blending MKO with base KO in varying proportions revealed a significant influence on both viscosity and the coefficient of friction (COF). Among the tested ratios, the 50% MKO blend exhibited the lowest COF, indicating an optimal balance between chemical reactivity and base oil properties for effective lubrication.

The study further investigated the effect of incorporating 0.025 wt% of functionalized hexagonal boron nitride (fh-BN) nanoparticles into the KO and KO-MKO blends. The addition of fh-BN notably improved the anti-wear and load-bearing characteristics of the oils, particularly under fully flooded and starved lubrication conditions. The nanoparticles facilitated the formation of a stable tribofilm on the metal surfaces, effectively reducing metal-to-metal contact and minimizing wear.

Friction-induced vibration analysis at the point of seizure provided mechanistic insights into lubricant failure. Pure KO exhibited a gradual increase in vibration energy, suggestive of progressive tribofilm degradation. In contrast, lubricants containing fh-BN nanoparticles demonstrated an abrupt failure, indicating a sudden breakdown of the

nanoparticle-reinforced tribolayer, which had remained intact under load until the point of failure.